Madelung potentials in disordered systems

1997 J. Phys.: Condens. Matter 9 5609

(http://iopscience.iop.org/0953-8984/9/26/009)

J. Phys.: Condens. Matter **9** (1997) 5609–5622. Printed in the UK PII: S0953-8984(97)81628-1

Madelung potentials in disordered systems

R J Cole and P Weightman

Department of Physics and Surface Science Research Centre, University of Liverpool, Liverpool L69 3BX, UK

Received 5 February 1997, in final form 25 March 1997

Abstract. We analyse the contribution of Madelung terms to the local potential on atomic sites in disordered alloys, and assess the extent to which the variation in the local potential should be observable in high-resolution x-ray photoelectron experiments. We show that a model in which the charge on an atom is determined by the global composition predicts considerable broadening of core-level photoelectron spectra. Such disorder broadening has not been observed experimentally. A model in which the local charge is determined by the number of 'unlike' nearest neighbours predicts a much smaller disorder broadening, but one which should be observable in high-resolution measurements for some alloy systems.

1. Introduction

The electrostatic energy of arrays of charges has attracted continued attention since the work of Madelung [1]. Elegant solutions to the Madelung problem exploiting the near cancellation of electrostatic effects at long range have continued to emerge [2–5], giving insight into a wide range of 'ionic' phenomena. The advent of electron spectroscopy stimulated renewed interest in Madelung potentials at crystal surfaces [6, 7], and the influence of Madelung energies on surface ordering and segregation has also been considered [8]. In recent years the inclusion of Madelung energies for disordered systems, usually implicitly assumed to be zero, has been shown to be essential to a truly *ab initio* description of the physical and electronic structure of random alloys [9]. A model in which the charge on a site is determined by the local composition has gained increasing support [10, 9] and has been used to explain the structural stability of a wide range of compounds and alloys [11].

In the present work we consider disorder effects in the total electrostatic potential (Madelung plus intra-atomic) of random alloys. One expects that variation in local bonding configuration will give rise to a distribution of potentials, and it is the aim of this work to predict the magnitude of this 'disorder broadening'. Since the core-level binding energy of an atom at site i in a solid measured with respect to the corresponding elemental solid can be written as

$$E_b^i = eV^i - E_R^i \tag{1}$$

where V^i is the potential at site i and E_R^i is the relaxation energy, disorder broadening of the electrostatic potential should be manifest in core-level photoelectron spectra. In the next section we consider two models for determining charges Q^i in disordered systems, and we investigate the distributions of the corresponding potentials using direct real-space summation of the Madelung series for finite clusters. This approach permits investigation of surface effects, relevant to x-ray photoelectron spectroscopy (XPS) experiments. The

0953-8984/97/265609+14$19.50

Madelung contribution to core-level binding energy shifts will also be briefly discussed. In section 3 we present XPS spectral simulations, and in section 4 we discuss the wider context of Madelung effects in disordered systems and consider how current charge models may be generalized.

2. Potentials and core-level binding energies

Following references [10] and [11] we model a random substitutional alloy by an array of charged spheres, each centred on a lattice point of the crystal structure. For simplicity we set the atomic radii as $R/2$ where R is the nearest-neighbour distance. The potential at lattice point i in the alloy relative to the corresponding elemental solid is then

$$V^i = \frac{14.4}{R}\left\{2Q^i + \sum_{m=1}^{\infty}\frac{1}{\rho_m}\sum_{j\in m}Q^j\right\} \tag{2}$$

where the first term is the intra-atomic term and the second term is the Madelung potential. If the charges Q^j are measured in units of e, the electronic charge, and all distances are in Å, then the potential is in volts. (We suppress the 14.4 factor in subsequent equations for brevity.) The first summation in the Madelung term is over concentric spheres with radius $R\rho_m$ centred on site i, and the second is over the Z_m sites in the mth shell.

We consider an unspecified crystal lattice populated with A and B atoms and asign an occupation variable S^i to each site such that $S^i = -1$ $(+1)$ if i is occupied by an A (B) atom. If the alloy is perfectly random there is no correlation in the S^i. To characterize the distribution of potentials in the random alloy we first require a model for the charge at each site.

2.1. The fixed-charge model

We may suppose that the charge on a site i is determined by the composition fraction for the species type at that site, c^i. For a random binary alloy A_xB_{1-x}, charge neutrality requires

$$-Q^{\mathrm{A}}c^{\mathrm{A}} = Q^{\mathrm{B}}c^{\mathrm{B}} \tag{3}$$

where $c^{\mathrm{A}} = x$ and $c^{\mathrm{B}} = 1 - x$. We refer to this as the fixed-charge model (FCM) since the charges do not vary with the local environment but merely reflect global stoichiometry; all of the A atoms and separately all of the B atoms have the same charge. Given equation (3), the average potential for A (or B) sites with a particular number of 'unlike' nearest neighbours N_u is

$$\langle V(N_u)\rangle_{\mathrm{A\,(B)}} = \frac{Q^{\mathrm{A\,(B)}}}{R}\left(2 + Z_1 - \frac{N_u}{1 - c^{\mathrm{A\,(B)}}}\right) \tag{4}$$

where the angled brackets indicate averaging over all possible configurations of the alloy. In metallic alloys the degree of charge transfer is of the order of a tenth of an electron per atom [9]. Taking a nearest-neighbour distance R of 3 Å, equation (4) predicts on average a difference of approximately 1 eV in potential per unit change in N_u. This would imply considerable disorder broadening of core-level XPS spectra in random alloys, an expectation contradicted by experiment. We conclude that the FCM does not give a useful description of charges in disordered systems.

Table 1. Structural parameters for the FCC, SC, BCC and diamond lattices.

		m							
		1	2	3	4	5	Σ	X	Y
FCC							8.22	66.72	−3.56
	ρ_m	1	$\sqrt{2}$	$\sqrt{3}$	2	$\sqrt{5}$			
	Z_m	12	6	24	12	24			
	K_m	4	4	2	1	0			
BCC							4.93	33.12	−2.14
	ρ_m	1	$2\sqrt{\frac{1}{3}}$	$2\sqrt{\frac{2}{3}}$	$\sqrt{\frac{11}{3}}$	2			
	Z_m	8	6	12	24	8			
	K_m	0	4	2	0	1			
SC							3.33	20.04	−1.34
	ρ_m	1	$\sqrt{2}$	$\sqrt{3}$	2	$\sqrt{5}$			
	Z_m	6	12	8	6	24			
	K_m	0	2	0	1	0			
Diamond							0.92	16.64	−2.16
	ρ_m	1	$2\sqrt{\frac{2}{3}}$	$\sqrt{\frac{11}{3}}$	$4\sqrt{\frac{1}{3}}$	$\sqrt{\frac{19}{3}}$			
	Z_m	4	12	12	6	12			
	K_m	0	1	0	0	0			

2.2. The correlated-charge model

Chemical wisdom suggests that an atom surrounded by all 'like' atoms will be approximately neutral while an atom bonded to all 'unlike' atoms will experience the maximum possible charge transfer. This means that the *charges* in a random system are correlated even when the *site occupations* are truly random. Magri *et al* have suggested [10] a correlated-charge model (CCM) with the form

$$Q^i = \lambda \sum_{j \in \mathrm{nn}^i} (S^i - S^j) = 2\lambda N_u S^i \tag{5}$$

where λ determines the ionicity and nn^i denotes the set of sites that are nearest neighbours of site i. The intra-atomic contribution to $V^i(N_u)$ is independent of configuration by assumption, and so $\langle V(N_u)\rangle$ can be written as

$$\langle V(N_u)\rangle_{\mathrm{A\,(B)}} = \frac{4\lambda N_u}{R} S^{\mathrm{A\,(B)}} + \frac{1}{R}\sum_{m=1}^{\infty} \frac{1}{\rho_m} \langle Q_m(N_u)\rangle_{\mathrm{A\,(B)}} \tag{6}$$

where

$$\langle Q_m(N_u)\rangle_{\mathrm{A\,(B)}} = \left\langle \sum_{j \in m} Q^j \right\rangle. \tag{7}$$

Choosing a central site and its nearest-neighbour composition amounts to fixing the S^j for $j \in \mathrm{nn}^i$. This influences the charges of these sites both directly, since they all have by definition site i as a neighbour, and indirectly since a number of these sites are also mutual nearest neighbours. Substitution of equation (5) into equation (7) yields

$$\langle Q_1(N_u)\rangle_{\mathrm{A\,(B)}} = 2\lambda S^{\mathrm{A\,(B)}} Z_1(Z_1 - 1 - K_1)(1 - c^{\mathrm{A\,(B)}}) - 2\lambda S^{\mathrm{A\,(B)}}(Z_1 - K_1)N_u \tag{8}$$

where K_m is the number sites that are simultaneously nearest neighbours of the central site and a site in the mth shell [9]. The choice of i and its nearest-neighbour composition does not impose any selection criteria on the site occupations of any subsequent shells, but any shell containing sites which share nearest neighbours with the central site (i.e. $K_m \neq 0$) still experience an indirect influence on their charge. For these shells we find

$$\langle Q_{m>1}(N_u)\rangle_{\mathrm{A\,(B)}} = 2\lambda S^{\mathrm{A\,(B)}} K_m Z_m \left[c^{\mathrm{A\,(B)}} - 1 + \frac{N_u}{Z_1} \right]. \tag{9}$$

All shells with $K_m = 0$ are on average charge neutral and do not contribute to $\langle V(N_u)\rangle$. Equation (6) can now be rewritten:

$$\langle V(N_u)\rangle_{\mathrm{A\,(B)}} = 2\frac{\lambda}{R} S^{\mathrm{A\,(B)}} Z_1 (Z_1 - 1 - \Sigma)(1 - c^{\mathrm{A\,(B)}}) + N_u 2\frac{\lambda}{R} S^{\mathrm{A\,(B)}} (2 - Z_1 + \Sigma) \tag{10}$$

where Σ is the lattice-dependent constant defined by

$$\Sigma = \sum_{m=1}^{\infty} \frac{K_m Z_m}{\rho_m Z_1}. \tag{11}$$

Equation (10) has the form

$$\langle V(N_u)\rangle_{\mathrm{A\,(B)}} = \frac{\lambda}{R} \left[X(1 - c^{\mathrm{A\,(B)}}) + Y N_u \right] S^{\mathrm{A\,(B)}} \tag{12}$$

and so for a given lattice the average potentials are linear in N_u with gradient independent of composition. Values of K_m, Z_m, ρ_m, X and Y can be found in table 1 for various lattices.

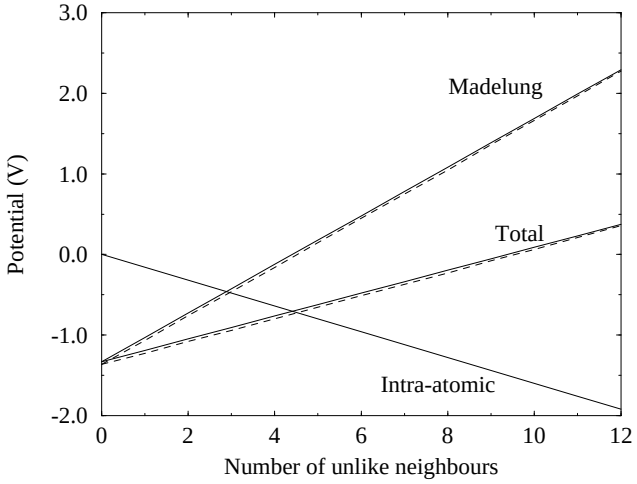

Figure 1. The variation of $\langle V(N_u)\rangle_{\mathrm{A}}$, the average potential for A sites with a given number of unlike nearest neighbours, with N_u for the $A_{0.5}B_{0.5}$ FCC lattice. The decomposition into intra-atomic and Madelung potentials is also shown. The solid lines are the analytic results while the dashed lines are results obtained numerically using a cluster.

The variation of $\langle V(N_u)\rangle_{\mathrm{A}}$ with N_u and its decomposition into intra-atomic and Madelung components are plotted in figure 1 for the random $A_{0.5}B_{0.5}$ FCC lattice, where values of $R = 3$ Å and $\lambda = 0.1/12$ (corresponding to an average charge of 0.1) were used. The Madelung part of $\langle V(N_u)\rangle_{\mathrm{A\,(B)}}$ scales faster with N_u than the intra-atomic part

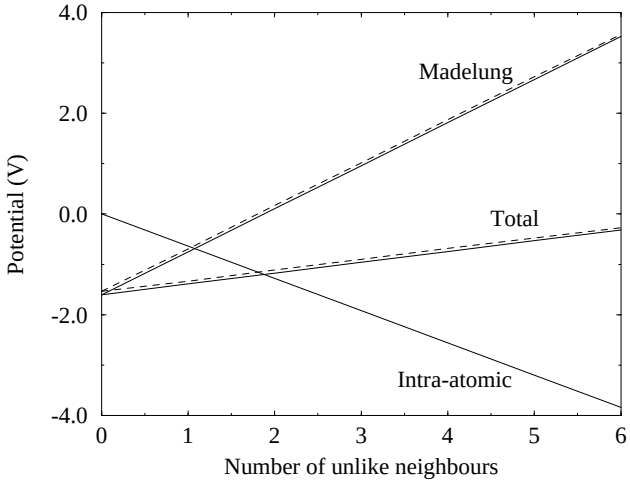

Figure 2. The variation of $\langle V(N_u)\rangle_A$, the average potential for A sites with a given number of unlike nearest neighbours, with N_u for the $A_{0.5}B_{0.5}$ SC lattice. The decomposition into intra-atomic and Madelung potentials is also shown. The solid lines are the analytic results while the dashed lines are results obtained numerically using a cluster.

but with opposite sign to $S^{A(B)}$, and so the total potential varies with $-N_u S^{A(B)}$ (i.e. Y is negative). For the chosen values of λ and R, Y' ($=14.4Y\lambda/R$), the gradient of $\langle V(N_u)\rangle$ against N_u, for the FCC lattice, is 0.14 eV, suggesting a modest disorder broadening of alloy core-level XPS spectra. Figure 2 shows the corresponding variation of $\langle V(N_u)\rangle$ with N_u for the disordered SC lattice. In this case $\lambda = 0.2/6$ was chosen to give a similar range of potentials as for the FCC lattice. Although no disordered alloys with an underlying SC lattice are known to exist, comparison of SC and FCC lattices reveals the dependence of disorder effects on the degree of 'openness' of the crystal structure.

2.3. Cluster calculations

Cluster calculations were performed to investigate the distributions of the $V^i(N_u)$ about their average values. When considering ordered crystals it is sufficient to calculate the Madelung potential at one site which may be chosen to be at the centre of a large cluster. To study the distribution of potentials in a disordered system one must sample over a sufficiently large number of sites for a reasonable number of configurations to be represented. On the other hand the sampled volume must be small compared to the cluster size so that the sampled sites are truly bulk-like. To get some indication of the feasibility of this procedure we first considered a cube-shaped SC cluster with (001) surfaces comprising 30^3 sites and populated to give the rock-salt structure. Since the standard Evjen procedure [12] is not applicable to disordered systems, the surface charges for the rock-salt structure were determined using equation (5) for consistency. At the centre of the cluster we found the correct Madelung potential to within an accuracy of 1 in $\sim 10^8$, and this value was preserved to 1 in $\sim 10^5$ within ten lattice parameters of the centre. The 'CCM-terminated' surface was found to greatly aid convergence of the Madelung potential with respect to cluster size, very much in the spirit of the Evjen termination. These results for the ordered system provide a guide for the size of cluster and sampling volume one would like to use for the disordered case.

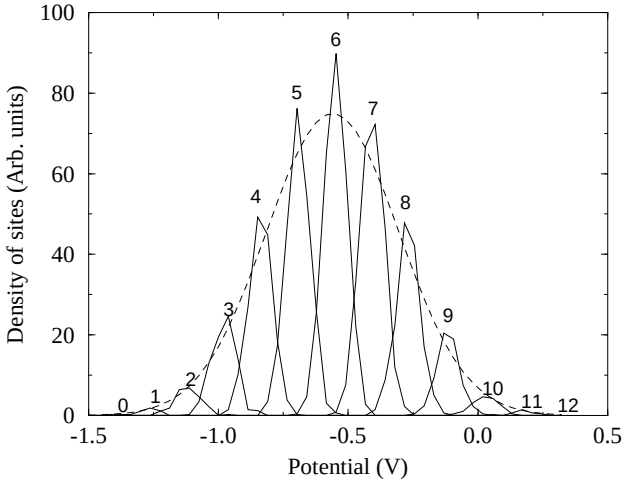

Figure 3. Each solid curve shows the distribution of potentials obtained for an $A_{0.5}B_{0.5}$ FCC cluster for the indicated value of N_u. The dashed curve is a Gaussian distribution with FWHM given by 4.2 times the component separation.

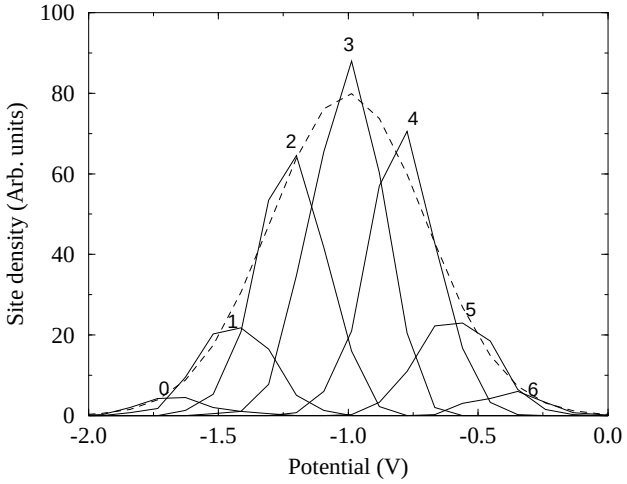

Figure 4. Each solid curve shows the distribution of potentials obtained for an $A_{0.5}B_{0.5}$ SC cluster for the indicated value of N_u. The dashed curve is a Gaussian distribution with FWHM given by 3.5 times the component separation.

While preserving composition, disorder was then introduced into the site occupations, and all charges in the system were determined according to equation (5). The potentials at sites within ten lattice parameters from the centre of the cluster were then calculated. The calculation was repeated for an FCC $A_{0.5}B_{0.5}$ cluster. For both structures, λ and R were given the values used in the previous subsection. Values of $\langle V(N_u)\rangle_A$ calculated for disordered FCC and SC clusters are compared with the analytical results from equation

(10) in figures 1 and 2 respectively. We find that the CCM clusters give the correct N_u-dependence for the average potentials, and also their absolute magnitude to a reasonable approximation. We may attribute this latter observation to the local charge neutrality implicit in equation (5). Local charge neutrality ensures that all shells outside the sampling volume are nearly charge neutral for any given cluster configuration. In the FCM this condition would only be met by configurational averaging, and large fluctuations would be expected between the absolute potentials within sampling volumes of different particular clusters.

The accuracy of the CCM cluster results for $\langle V(N_u)\rangle$ suggests that the clusters should also give a good description of the *distributions* of the $V^i(N_u)$ about these averages. These distributions are shown in figures 3 and 4 for the FCC and SC structures respectively. For any given N_u we find $V^i(N_u) \approx \langle V(N_u)\rangle_{\mathrm{A\,(B)}}$ $\forall i = \mathrm{A\,(B)}$. Thus the core potential at a site is determined predominantly by the composition of its nearest-neighbour shell. The calculated distributions for each N_u are found to be Gaussian with FWHM smaller than the gradient Y' (i.e. the component splitting in figure 3) for the FCC lattice. For the SC lattice the component broadening and component splitting are comparable. Comparison with the Gaussians in figures 3 and 4 (given by the dashed curves) shows that the overall effect of disorder is an approximately Gaussian broadening. It can be seen that the component broadening is a much greater fraction of the overall broadening for the more open SC lattice.

2.4. Binding energy shifts

We recall that for an ordered system a chemical shift in core-level photoelectron binding energy relative to the corresponding elemental solid can be expressed in the form [13]

$$\Delta E_b^{\mathrm{A\,(B)}} \approx e\,\Delta V^{\mathrm{A\,(B)}} = e\,\Delta Q^{\mathrm{A\,(B)}}\left(\frac{2}{R} - \frac{\alpha}{R}\right) \tag{13}$$

where α is the Madelung constant and the approximation in the first equality is due to the neglect of relaxation energy shifts. We now derive the equivalent expression for a random alloy within the CCM.

The probability of a site having a given number of unlike neighbours is

$$P(N_u) = \frac{Z_1!}{(Z_1 - N_u)!N_u!}(c^{\mathrm{A\,(B)}})^{Z_1 - N_u}(1 - c^{\mathrm{A\,(B)}})^{N_u}. \tag{14}$$

The average A (B) site charge (when no constraint on N_u is enforced) is therefore

$$\bar{Q}^{\mathrm{A\,(B)}} = 2\lambda S^{\mathrm{A\,(B)}} \sum_{N_u=0}^{Z_1} P(N_u)N_u = 2\lambda S^{\mathrm{A\,(B)}} Z_1(1 - c^{\mathrm{A\,(B)}}). \tag{15}$$

The average charge in the first shell is then

$$\bar{Q}_1 = \sum_{N_u=0}^{Z_1} P(N_u)\langle Q_1(N_u)\rangle = -2\lambda S^{\mathrm{A\,(B)}} Z_1(1 - c^{\mathrm{A\,(B)}}) \tag{16}$$

while for subsequent shells we find

$$\bar{Q}_{m>1} = \sum_{N_u=0}^{Z_1} P(N_u)\langle Q_{m>1}(N_u)\rangle = 0.$$

Thus we find that there is on average a charge of $-\bar{Q}^{\mathrm{A\,(B)}}$ in the first shell, while all subsequent shells are on average charge neutral, implying perfect screening (on average) in the first shell.

Using equations (15)–(17) we obtain

$$\bar{V}^{\mathrm{A\,(B)}} = 2\frac{\lambda}{R}S^{\mathrm{A\,(B)}}Z_1(1 - c^{\mathrm{A\,(B)}}) = \frac{\bar{Q}^{\mathrm{A\,(B)}}}{R} \tag{17}$$

indicating a linear dependence of the core-level binding energy on composition [14]. By analogy with equation (13), the effective Madelung constant for disordered alloys within the CCM is $\alpha^{eff} = 1$ for all lattices and for all compositions. Shells with $m > 1$, $K_m \neq 0$ contribute to the average Madelung energy but do not contribute to the average potential $\bar{V}$. Clearly for disordered systems a distinction must be made between Madelung constants corresponding to the electrostatic *potential* and the electrostatic *energy*. For the CCM, Magri *et al* [10] have shown that the energy constant exhibits a parabolic variation with composition.

These results may be contrasted with those for the FCM. In the FCM all shells are on average neutral on account of global charge neutrality, and so there is no screening of the central site. Madelung effects then vanish on average (i.e. $\alpha^{eff} = 0$).

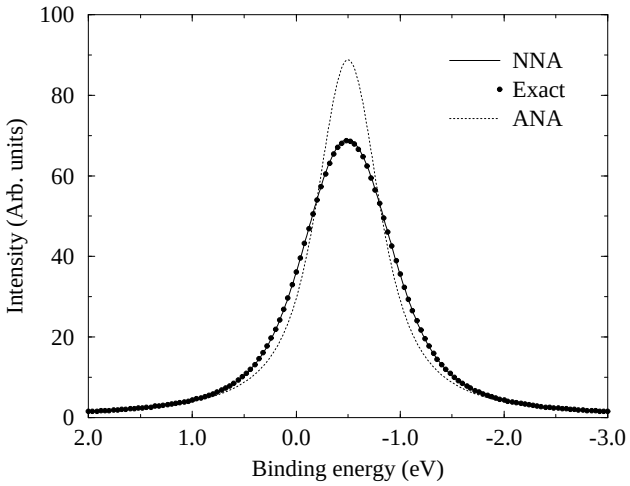

Figure 5. Comparison of exact (circles), NNA (solid curve) and ANA (dotted curve) simulated XPS spectra for the random FCC lattice.

3. Core-level XPS spectra

3.1. Spectral simulation

In this section we use the potentials calculated for the $A_{0.5}B_{0.5}$ FCC cluster to simulate XPS spectra using the expression

$$\langle f^i(\omega)\rangle_{\mathrm{A\,(B)}} = \frac{1}{N_{\mathrm{A\,(B)}}}\sum_{i=\mathrm{A\,(B)}} L^W(\omega, V^i) \tag{18}$$

where $N_{\mathrm{A\,(B)}}$ is the number of A (B) sites and where we have assumed that the component spectra $f^i(\omega)$ are given by $L^W(\omega, V^i)$, Lorentzians with FWHM W and position determined

by V^i, the potential at site i. The more compact expression

$$\langle f^i(\omega)\rangle_{\mathrm{A\,(B)}} \approx \sum_{N_u=0}^{Z_1} P(N_u) L^W(\omega, \langle V(N_u)\rangle_{\mathrm{A\,(B)}}) \tag{19}$$

where $P(N_u)$ is the probability of a site having a given N_u, is suggested by the demonstration in section 2 that the V^i are determined primarily by the composition of the nearest-neighbour shell. We refer to this expression as the 'nearest-neighbour approximation' (NNA). A further approximation

$$\langle f^i(\omega)\rangle_{\mathrm{A\,(B)}} \approx L^W(\omega, \bar{V}^{\mathrm{A\,(B)}}) \tag{20}$$

referred to as the 'average neighbour approximation' (ANA) assumes a single effective A (B) environment which experiences the average potential $\bar{V}$. Comparison of $f^i(\omega)$ determined using equations (15) (exact) and 17 (ANA) will determine explicitly the extent of disorder broadening. Comparison of equations (15)–(17) is made in figure 5 for the FCC cluster, where $W = 0.6$ eV and a Gaussian broadening of $\Gamma = 0.3$ eV FWHM were used to simulate lifetime broadening and experimental resolution respectively. For the parameters used, disorder can be seen to significantly broaden the core spectrum. We find that the 13-component envelope generated by the NNA performs extremely well. Furthermore the small 'missing' Gaussian broadening could be explicitly added to the NNA spectrum to recover essentially the exact result.

Core-level XPS spectra of disordered alloys have usually been performed with monochromated Al Kα radiation with an experimental resolution of about 0.5 eV. While chemical shifts in core-level binding energies are routinely observed, alloy core-level spectra have previously been interpreted in terms of a single bulk component. The results in figure 5 show that 'third-generation' XPS spectrometers, which achieve an experimental resolution of about 0.25 eV with a high photon flux, should be capable of observing disorder broadening of XPS lines in alloys with narrow core levels.

3.2. Surface effects

In simulating the XPS experiment we must consider surface effects. We consider first the surface of the ordered SC cluster described in section 2.3. With the NaCl bond length of 2.82 Å and assuming that bulk and surface sites have unit ionicity we obtain a reduction of the anion core-level binding energy of 0.339 eV at the (001) surface, in excellent agreement with previous work [6, 7]. Reducing the surface ionicity to $5/6$ in the spirit of the CCM we obtain a Madelung shift of 1.712 eV but a counter shift in the intra-atomic term of 0.851 eV giving a reduction in the surface core-level binding energy of 0.861 eV. The tendency for the CCM termination to enhance surface core-level shifts in ordered systems has been pointed out previously by Watson *et al* [7]. For the subsurface layer we obtained a potential shift of -0.004 eV for unit surface ionicity and 0.053 eV for the CCM termination. In the next layer down the shifts were two orders of magnitude smaller. This rapid decay of surface effects with depth is confirmed by the general experimental observation of only bulk and surface features in core-level XPS.

Calculated average potentials for the surface and subsurface sites of the disordered SC cluster are compared with the bulk averages in figure 6. As for the ordered alloy, we find that the subsurface layer is essentially bulk-like while the surface potentials have a shallower N_u-dependence. Bulk, surface and subsurface potentials had very similar distributions about their respective averages. These results suggest that XPS spectra are well represented by the superposition of a bulk and a surface NNA envelope, each defined by the single parameter

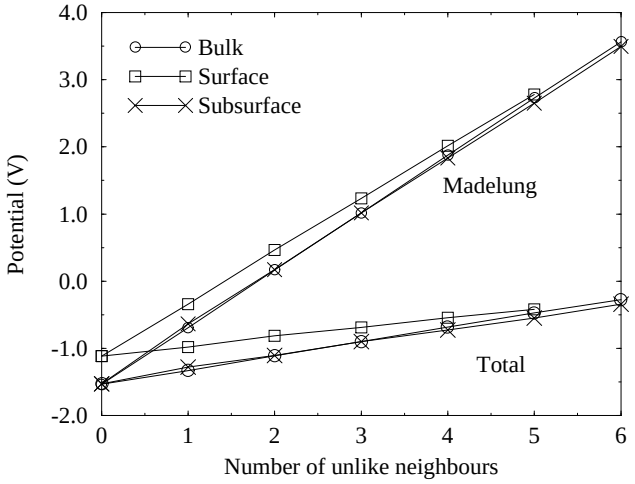

Figure 6. Calculated average potentials for a SC cluster for bulk, surface and subsurface sites as functions of N_u.

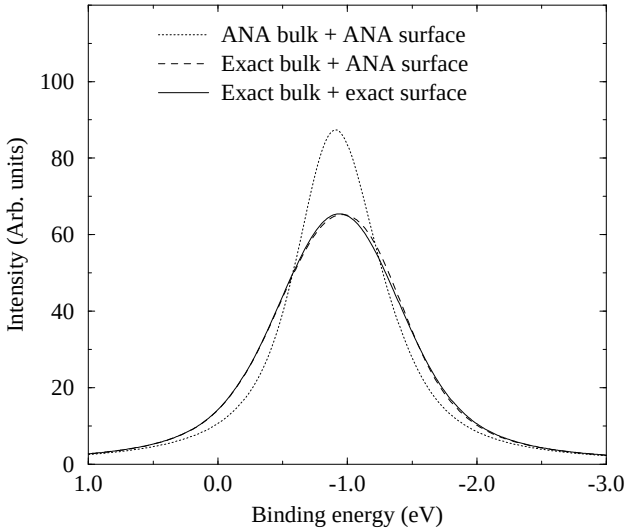

Figure 7. Simulated XPS spectra for the disordered SC(001) surface using (i) exact bulk plus exact surface (solid curve), (ii) exact bulk plus ANA surface (dashed curve), and (iii) ANA bulk plus ANA surface (dotted curve) components.

λ. However, we recall that the bulk–surface distinction made by the potentials in the CCM cluster provides only the modification of the surface Madelung contribution to surface core-level shifts in partially ionic systems, and provides no insight into the surface core-level shifts already present in elemental solids. This uncertainty in the surface contribution may be expected to confuse the unambiguous identification of core-level disorder broadening. To address this point we have performed the three simulations shown in figure 7. The three curves were obtained using (i) exact bulk plus exact surface (solid curve), (ii) exact bulk

plus ANA surface (dashed curve), and (iii) ANA bulk plus ANA surface (dotted curve) components. In each case the surface intensity was 15% of the bulk intensity. An arbitrary -0.5 eV shift was added to the surface component to represent that contribution to the surface core-level shift also present in elemental solids. Other values were also tried but gave no new effects. It can be seen that the total spectrum is insensitive to the surface disorder broadening. We found that the effect of bulk disorder broadening could not be reproduced by varying the energy of the surface component in the 'bulk(ANA)+surf(ANA)' simulation. We conclude that for relatively weak surface emission we do not expect surface effects to present a fundamental barrier to the experimental observation of bulk disorder broadening of core-level XPS spectra.

4. Discussion

So far we have pointed out that the phenomena of disorder broadening in the core-level XPS spectra of random alloys should be observable using high-resolution instruments. We have predicted the magnitude of this effect based on the correlated-charge model of equation (5) and estimates of the 'charge-transfer' parameter λ. In this section we discuss the validity and context of the CCM and justify the choices of λ. We will also comment on the possible generalization of the CCM.

4.1. The validity of the CCM

Over the last decade, band-structure methods based on the coherent potential approximation (CPA) in which a single A (B) atom is embedded in an effective medium have been found to provide the best available description of the electronic structure of random substitutional binary alloys [17]. In spite of its apparent success, the CPA is a single-site theory omitting Madelung contributions to the total energy by construction, and so yields unreliable structural properties for alloys with non-negligible charge transfer [9].

To address this shortcoming, Johnson and Pinski [18] have developed the 'charge-correlated CPA' (cc-CPA). In this approach the charge on a site i is assumed to be determined solely by the number of unlike neighbours N_u, although no assumption of linearity is made. In this way the cc-CPA becomes a '(Z_1+1)-site' theory. By adding the electrostatic energy due to the interaction of $Q^{i=\mathrm{A\,(B)}}(N_u)$ with $\langle V(N_u)\rangle_{\mathrm{A\,(B)}}$, the average potential shift for each value of N_u, to the energy functional of the standard CPA, Johnson and Pinski observed [18] a dramatic improvement in the formation energies of several alloys. They also found that the self-consistently determined charges for the Z_1+1 components were linear in N_u and with gradient independent of composition x. Transferability appeared to hold even to the impurity limit. These results lend great support to the CCM of Magri *et al* [10] given in equation (5).

Given its success, Johnson and Pinski [18] then used the cc-CPA to develop a modified single-site theory. The so-called screened CPA (scr-CPA) is obtained by considering a single site experiencing the average electrostatic potential $\bar{V}$. The scr-CPA was found to incorporate most of the Madelung energy of the cc-CPA at greatly reduced computational cost. We may draw a conceptual parallel between cc-CPA and scr-CPA and the NNA and ANA models for core XPS spectra.

A similar single-site theory, referred to as SIM-CPA, has also been developed [19]. Though based on similar physics, this model and the scr-CPA gave rise to Madelung energies differing by a prefactor β. The apparent discrepancy has been explained by Korzhavyi *et al* [20] who pointed out that the energy corrections in both models were approximate. By

scaling the Madelung correction to reproduce thermodynamical properties of a number of alloys, the optimum prefactor was found [20] to lie between 0.5 (the scr-CPA result) and 1.0 (the SIM-CPA result). Magri *et al* [10] have shown that equation (5) for an array of point charges yields an exact Madelung correction with $\beta = 0.657$, consistent with the analysis of Korzhavyi *et al* [20]. These comparisons with first-principles calculations have confirmed the validity and importance of point charge electrostatics and a simple charge-transfer picture embodied in the CCM.

4.2. Estimates of λ

There is justified reluctance for solid-state physicists to speak of 'charge transfer', as this does not constitute a quantum mechanical observable and the concept is therefore vague and arbitrary. Nonetheless the concepts of electronegativity and ionicity have had great historical importance in chemistry [21, 22] and if used with care can provide a compact description of electronic structure and bonding. Indeed Wolverton and Zunger have very recently shown [11] how the charge-transfer picture can be used to explain the structural stability of a wide range of compounds and alloys. These authors pointed out that although any real-space charge partition scheme is necessarily arbitrary, the electrostatic energy in first-principles calculations is well defined. One can then estimate λ by collapsing the charge density onto the lattice sites so that the electrostatic energy of the resulting point charge array reproduces that of first-principles calculations. In this way Wolverton and Zunger obtained [11] $\lambda \sim 0.006$ for CuPd and CuZn alloys. Combining this value with the Cu lattice parameter we obtain $\lambda/R \sim 0.0024$. This closely corresponds to the parameters used throughout the present work for the FCC calculations. With the present value of λ/R equation (14) predicts a shift in Cu 2p binding energy of up to 1 eV in Cu_xPd_{1-x} alloys, in broad agreement [14] with experiment [23–25]. Thus our choice of parameters seems sound and should be particularly relevant to Cu_xPd_{1-x} alloys. Likewise the bulk-to-surface intensity ratio and lifetime broadening used in section 3 were chosen to correspond to that for the Cu 2p core level [26]. We suggest that the Cu 2p line in the Cu_xPd_{1-x} alloy system provides a suitable test case for the experimental identification of the disorder broadening of core-level XPS spectra of random alloys. Preliminary results for this alloy system [27] are in accord with the present theoretical work and provide experimental confirmation of the presence of disorder broadening in core-level XPS spectra.

Wolverton and Zunger [11] identify a number of alloy systems with larger ionicity (e.g. Cu_xAu_{1-x}, Ni_xAl_{1-x} and Li_xAl_{1-x}) which may exhibit more pronounced disorder broadening. However, there will be an increased tendency for short-range ordering with increasing λ, and since V^i is determined primarily by N_u it is clear that short-range ordering will quench disorder broadening extremely efficiently.

4.3. The bond ionicity model

Most of the evidence lending support to the CCM description of charges in alloys is derived from close-packed FCC alloys. Any description in terms of only the nearest-neighbour shell will deteriorate as the coordination number Z_1 is reduced, as atoms will 'see' more remote atoms between the gaps in the first shell. It should then be expected that the validity of the CCM decreases with the 'openness' of the lattice. This has very recently been demonstrated by explicitly comparing calculated charges and potentials obtained from *ab initio* calculations for large disordered clusters with the predictions of the CCM [28, 29]. It was found that the CCM description of the electrostatics in random alloys is extremely

good for FCC alloys, but less accurate for BCC systems [28, 29].

Another weakness of the CCM is the neglect of direct correlation between 'like' charges. For example, one may expect a tendency for a charged A atom to share some of its excess charge with any neighbouring neutral A atoms. We may also expect some deviation from the linear scaling of charge transfer between unlike neighbours with N_u. For example one may expect the difference in charge between sites with $N_u = 0$ and 1 to be greater than that between sites with $N_u = Z_1 - 1$ and Z_1. The dependence of elemental electronegativities on charge state is well known [22], and can be expressed as

$$\chi^i = \chi_0^i + \eta^i Q^i. \tag{21}$$

If we define the ionicity of a bond between two adjacent atoms $I(i, j)$ as their electronegativity difference, we may suppose the charge on a site is given by the sum of its bond ionicities:

$$Q^i = \sum_{j \in \mathrm{nn}^i} I(ij) = \sum_{j \in \mathrm{nn}^i} (\chi_0^j - \eta^j Q^j - \chi_0^i + \eta^i Q^i). \tag{22}$$

In the $\eta^{\mathrm{A}}, \eta^{\mathrm{B}} \to 0$ limit we recover the CCM with $2\lambda S^i \equiv \chi_0^j - \chi_0^i$. With $\eta^{\mathrm{A}}, \eta^{\mathrm{B}} \neq 0$ equations (18) and (19) must be solved iteratively to achieve self-consistency. Nonetheless this generalization of the CCM retains the simplicity and intuition of basic chemical concepts. We expect the bond ionicity model (BIM) given by equations (18) and (19) to reduce the variation in charge in a disordered system and so maintain an even greater degree of local charge neutrality than the CCM.

5. Summary

We have discussed the correlated-charge model in which the charge on any site is assumed to be proportional to its number of unlike neighbours N_u. We have shown that the average potential at a site with a given N_u is also proportional to N_u. The small amount of scatter about these averages is Gaussian in character and increases with the openness of the crystal structure. Averaging out the N_u-dependence, we showed that $\bar{V}^{\mathrm{A\,(B)}}$, the potential averaged over all A (B) sites, is given by $\bar{Q}/R$, corresponding to an effective Madelung constant of 1 for all structures and all compositions. Using a realistic estimate of the model parameter λ we have shown that disorder broadening of core-level XPS lines in random alloys should be observable with the resolution afforded by current XPS spectrometers. Conversely, if disorder is not observed, XPS should be a indication of the presence of short-range order. The 'nearest-neighbour approximation', in which the XPS spectrum is given by the superposition of $Z_1 + 1$ components, was found to give an excellent description of the XPS lineshape of disordered alloys. A model generalizing the CCM model for the charges in random alloys was also presented.

References

[1] Madelung E 1918 *Z. Phys.* **19** 524
[2] Ewald P 1921 *Ann. Phys., Lpz.* **64** 253
[3] Lennard-Jones J E and Dent B M 1928 *Trans. Faraday Soc.* **24** 92
[4] Evjen H M 1932 *Phys. Rev.* **39** 675
[5] Wolf D 1992 *Phys. Rev. Lett.* **68** 3315
[6] Parry D E 1975 *Surf. Sci.* **49** 433
[7] Watson R E, Davenport J W, Perlman M L and Sham T K 1981 *Phys. Rev.* B **24** 1791
[8] Borici A and Monnier R 1993 *Phys. Rev.* B **47** 6768

[9] See, for example,
Zunger A 1994 *Statics and Dynamics of Alloy Phase Transformations* ed P E A Turchi and A Gonis (New York: Plenum) pp 361–419
Johnson D D and Pinski F J 1994 *Metallic Alloys: Experimental and Theoretical Perspectives* ed J S Faulkner and R G Jordan (Dordrecht: Kluwer) pp 149–58
[10] Magri R, Wei S H and Zunger A 1990 *Phys. Rev.* B **42** 11 388
[11] Wolverton C and Zunger A 1995 *Phys. Rev.* B **51** 6876
[12] Kittel C 1986 *Introduction to Solid State Physics* 6th edn (New York: Wiley)
[13] Gelius U 1973 *Phys. Scr.* **9** 133
[14] We note that the linear dependence of $\bar{V}$ on c may not be strictly reproduced in experimentally determined core-electron binding energies due to the possibility of additional shifts induced by changes in the surface dipole potential, relaxation energies and valence configuration changes [15, 16] which have not been discussed here.
[15] Watson R E, Perlman M L and Herbst J F 1976 *Phys. Rev.* B **13** 2358
[16] Williams A R and Lang N D 1978 *Phys. Rev. Lett.* **40** 954
[17] See, for example,
Gyorffy B L, Johnson D D, Pinski F J, Nicholson D M and Stocks G M 1994 *Alloy Phase Stability* ed G M Stocks and A Gonis (New York: Plenum) p 293
[18] Johnson D D and Pinski F J 1993 *Phys. Rev.* B **48** 11 553
[19] Abrikosov I A, Vekilov Yu H, Korzhavyi P A, Ruban A V and Shilkrot L E 1992 *Solid State Commun.* **83** 867
[20] Korzhavyi P A, Ruban A V, Abrikosov I A and Skriver H L 1995 *Phys. Rev.* B **51** 5773
[21] Pauling L 1935 *Nature of the Chemical Bond* (Ithaca, NY: Cornell University Press)
[22] Phillips J C 1970 *Rev. Mod. Phys.* **42** 317
[23] Mårtensson N, Nyholm R, Callen H, Hedman J and Johansson B 1981 *Phys. Rev.* B **24** 1725
[24] Sundaram V S, de Moraes M B and Kleiman G G 1981 *J. Phys. F: Met. Phys.* **11** 1151
[25] Cole R J and Weightman P 1994 *Metallic Alloys: Experimental and Theoretical Perspectives* ed J S Faulkner and R G Jordan (Dordrecht: Kluwer)
[26] Citrin P H, Wertheim G K and Baer Y 1983 *Phys. Rev.* B **27** 3160
[27] Cole R J, Brooks N J and Weightman P 1997 *Phys. Rev. Lett.* **78** 3777
[28] Faulkner J S, Wang Y and Stocks G M 1995 *Phys. Rev.* B **52** 17 106
[29] Wolverton C, Zunger A, Froyen S and Wei S H 1996 *Phys. Rev.* B **54** 7843